ACS APPLIED MATERIALS & INTERFACES

Research Article

www.acsami.org

Gallic Acid Tailoring Surface Functionalities of Plasma-Polymerized Allylamine-Coated 316L SS to Selectively Direct Vascular Endothelial and Smooth Muscle Cell Fate for Enhanced Endothelialization

Zhilu Yang,*[,†,‡] Kaiqin Xiong,[†,‡] Pengkai Qi,[†,‡] Ying Yang,[†,‡] Qiufen Tu,[†,§] Jin Wang,*[,†,‡] and Nan Huang*[,†,‡]

[†]Key Laboratory of Advanced Technology for Materials of Education Ministry, [‡]The Institute of Biomaterials and Surface Engineering, School of Materials Science and Engineering, and [§]Laboratory of Biosensing and MicroMechatronics, Southwest Jiaotong University, Chengdu 610031, China

Supporting Information

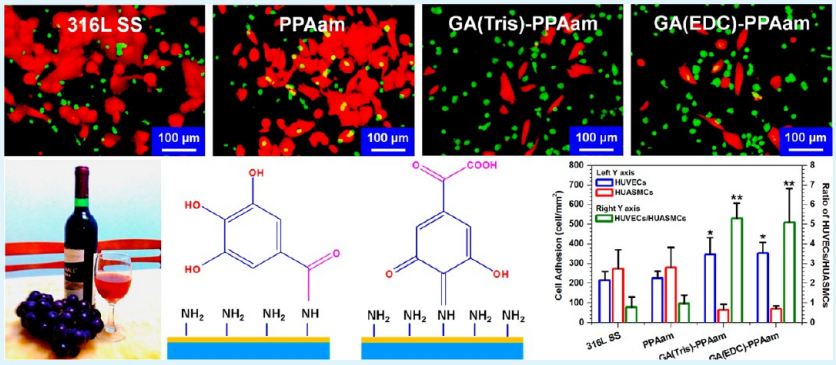

ABSTRACT: The creation of a platform for enhanced vascular endothelia cell (VEC) growth while suppressing vascular smooth muscle cell (VSMC) proliferation offers possibility for advanced coatings of vascular stents. Gallic acid (GA), a chemically unique phenolic acid with important biological functions, presents benefits to the cardiovascular disease therapy because of its superior antioxidant effect and a selectivity to support the growth of ECs more than SMCs. In this study, GA was explored to tailor such a multifunctional stent surface combined with plasma polymerization technique. On the basis of the chemical coupling reaction, GA was bound to an amine-group-rich plasma-polymerized allylamine (PPAam) coating. The GA-functionalized PPAam (GA-PPAam) surface created a favorable microenvironment to obtain high ECs and SMCs selectivity. The GA-PPAam coating showed remarkable enhancement in the adhesion, viability, proliferation, migration, and release of nitric oxide (NO) of human umbilical vein endothelial cells (HUVECs). The GA-PPAam coating also resulted in remarkable inhibition effect on human umbilical artery smooth muscle cell (HUASMC) adhesion and proliferation. These striking findings may provide a guide for designing the new generation of multifunctional vascular devices.

KEYWORDS: *gallic acid, plasma polymerization, endothelial cells, smooth muscle cells, competitive adhesion, vascular stent*

1. INTRODUCTION

Coronary artery diseases were mainly aroused by atherosclerosis and known as the leading killer in the modern society. The most regularly strategy for cardiovascular diseases therapy has been vascular stents. However, there were still fatal limitations after stenting of coronary atherosclerotic diseases, especially recurrent stenosis and late stent thrombosis (LST).[1,2] Drug eluting stents (DES), a useful tool with remarkable reduction in the stenosis rate,[3−5] has shown up and brought a new phase in modern interventional cardiology in the past decade. However, aimed at solving one problem, DES has been involved with considerably incremental risk of LST, which is still a catastrophic complication of consistently attached with lethality rates as high as 25%.[6] Current DES mainly focus on the inhibition of VSMC proliferation, however at the same time. They also suppress EC growth, resulting in a delayed endothelialization.[7]

Natural vascular endothelium is composed of monolayer ECs attached to the basement membrane of nanofibrillar and also the boundary between circulating blood and vessel wall barrier. ECs can adjust the balance of intravascular and VSMC growth as well as natural anticoagulant and maintain vascular patency. The creation of healthy endothelium on stent is a fatal factor to its success. The adhesion, survival, recruitment, spreading, proliferation, mobility behaviors of ECs play the crucial roles in arterial treatment and endothelium regeneration. Aiming to

Received: November 14, 2013
Accepted: January 31, 2014
Published: January 31, 2014

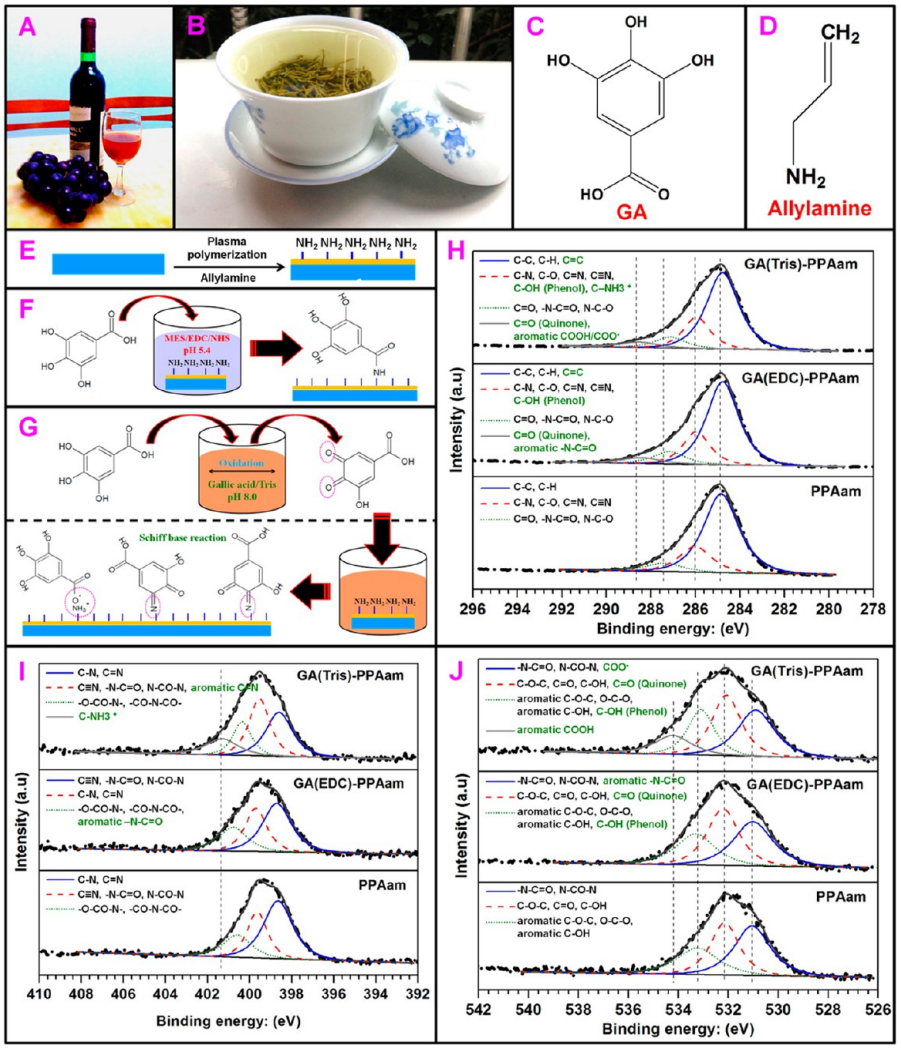

Figure 1. (A, B) Red wine and green tea rich in polyphenols. (C, D) Chemical structures of GA and allylamine. (E) Schematic illustration of the deposition of PPAam coating on 316L SS substrate. (F, G) Covalent conjugation of GA on the PPAam coating in WSC and Tris buffer solution respectively. (H) C1s, (I) N1s, and (J) O1s high-resolution spectra of the PPAam, GA(EDC)-PPAam, and GA(Tris)-PPAam surfaces.

improve the tissue/material interaction inducing accelerated endothelialization, researchers have been attempted numerous strategies of surface modification to develop healthy healing strategies because of stent deployment and vessel wall injury. This includes polymer coating,[8−10] and immobilization of VEGF,[11] proteins,[12] and cell recognition peptides.[13] However, largely current techniques paid their attentions on improving single aspects of vascular compatibility, promoting EC growth, while neglecting anticoagulant or antiproliferative effects. Therefore, considering minimal complications, a desired vascular stent should promote re-endothelialization while actively suppressing VSMC adhesion and proliferation. Peng et al.[14] found that TiO_2 nanotube coating could promote EC proliferation, migration, and function as well as inhibit the SMC proliferation. Nevertheless, Smith et al.[15] reported that this TiO_2 nanotube coating resulted in severe clotting and tended to delaminate. Many developments are needed to solve this obstacle.

Recently, more and more scholars have focused on depositing plasma polymerized coatings with amine groups to achieve the purpose of vascular stents modification,[12,16−18] as these thin, compact, and homogeneous coatings show strong adhesive interaction with substrates. Waterhouse et al.[16] have reported a stent with a durable, nondelaminating plasma-polymerized coating decorated with recombinant human tropoelastin, which exhibits multifaceted biocompatibility, is nonthrombogenic, and enhances EC proliferation. Our previous work also found that the plasma polymerized allylamine coating equipped with heparin exhibits a promising modification of a vascular stent.[17] Thus, immobilization of biomolecules with multifaceted functions on this type of plasma-polymer-coated stent may be a promising approach to address issues of re-endothelialization and restenosis.

However, only a few biomolecules possess ideal physiological reaction for vascular cells. A potential candidate is GA (3,4,5-triphydroxyl-benzoic acid), an important anticarcinogen.[19] It is a natural plant polyphenyl product derived from green teas and red wines and is highly rich in processed beverages.[20,21] GA also has other various biological activities including antibacterial,[22] antiviral,[23] and anti-inflammatory activity.[24] In addition to this, being a strong natural antioxidant, it has arterioprotective properties.[25] The antitumoral activity of GA is mainly attributed to its character of inducing apoptosis.[26,27] Of special importance is that Qiu et al.[28] found that GA could induce VSMC death, whereas GA was reported to show no cytotoxicity against normal ECs.[29] Such specific biological

characters of GA are positive to promote re-endothelialzation of vascular stent.

This work was aimed to construct a multifunctional stent coating which shows high vascular cell selectivity. GA has been thereby chosen to tailor the surface functionalities of PPAam coated 316L stainless steel (316L SS) stents, one of the most popular vascular stent materials. As reported, the effects of polyphenol including GA or its derivate on EC and SMC growth behavior were based on the functions of the carboxyl/galloyl and phenolic hydroxyl groups and the concentration of GA.[28,30−37] In addition, some researcher found that carboxyl/galloyl and phenolic hydroxyl groups of these polyphenol presented different influence on the growth behavior of SMCs.[35−37] Hereon, to investigate the effects of the functional groups of GA on EC and SMC growth, two different ways were used to immobilize GA on PPAam. The first one was involved in an active ester bonding of the primary amine group of PPAam with activated carboxylic groups of GA in water-soluble carbodiimide (WSC) (Figure 1F, the phenolic hydroxyl groups of GA could be well retained). The other is based on a Schiff base reaction of quinone groups of GA with the amine groups of PPAam in alkaline Tris buffer (Figure 1G, the carboxylic group of GA could be well retained). In this work, the effects of GA-PPAam coating on vascular cells were investigated by systemic evaluation of the performance of HUVECs and HUASMCs on the surface.

2. EXPERIMENTAL SECTION

PPAam Coating. The PPAam coating was deposited on 316L SS by using a pulsed radio frequency (RF) plasma polymerized equipment. The preparation and detailed deposition parameter was shown elsewhere.[38,39]

GA Conjugation. In this work, GA (Figure 1C) was conjugated on the PPAam coating using two different covalent reaction mechanisms. The first one is due to an active ester conjugation of the primary amine group on PPAam surface with the activated carboxylic group of GA in WSC (mark as GA(EDC)-PPAam). The other is based on a Schiff base reaction of quinone groups derived GA with the amine group of PPAam in Tris buffer (pH 8.5) (mark as GA(Tris)-PPAam). For the GA(EDC)-PPAam preparation, the 316L SS coated with PPAam coatings were added into 1 mg of GA (Purity ≥97.0%, Jinshan Reagents Company, Chengdu, China) per 1 mL of WSC solution.[39] In the case of the GA(Tris)-PPAam preparation, the 316L SS coated with PPAam films were immersed into a freshly prepared solution of 1 mg of GA per 1 mL of Tris (2 mg/mL, Purity ≥99.0%, Sigma, pH 8.5). After reaction for 12 h, both of the GA(EDC)-PPAam and GA(Tris)-PPAam were washed with PBS and distilled water in sequence.

X-ray Photoelectron Spectroscopy (XPS) Measurement. The surface chemical composition of the specimen were analyzed by XPS (XSAM800, Kratos Ltd., UK).[39]

Infrared (IR) Measurements. Grazing incidence attenuated total reflection Fourier transform infrared spectroscopy (GATR-FTIR) measurement was performed to analyze the chemical structure of the PPAam, GA(EDC)-PPAam, and GA(Tris)-PPAam using Nicolet model 5700 instrument.

HUVEC and HUASMC Culture. HUVECs and HUASMCs were derived from human umbilical vein. The detailed processes of cell culture were shown elsewhere.[39]

Adhesion, Viability and Proliferation of HUVECs. Actin immunostaining of HUVECs was used for the analysis of the cell morphology. The cell culture time was respectively 2, 24, and 72 h. The determination of the cell apoptosis or necrosis of cells was carried out to analyze the viability of the cells. Cell Counting Kit-8 (CCK-8) was used for the analysis of cell proliferation. The culture of HUVECs was carried out at a density of 5×10^4 cells/cm^2. The culture time of cell viability and proliferation was chosen as 1 and 3 days. The cell tests and statistical analysis of cell morphology were described in detail elsewhere.[39]

HUVEC Migration Assay. Migration of the healthy ECs from natural endothelium to a stent is crucial to in situ re-endothelialization. To address the issue associated with the damage of surface properties of the detected specimen caused by Scarification method (a common means to test cell migration), a new method has been reported in our previous work.[39] In this work, the same method was used to determine the HUVEC migration.

NO Release of Adherent HUVECs. NO release by ECs is a very important parameter to test the function of ECs. In this work, a common method of Griess reagent was used to determine the release level of NO produced by HUVECs. Breifly, the specimens were first cultured in medium containing HUVECs at high density of 5×10^5 cells/cm^2 for 8 h to rapidly form a compact cell monolayer that mimicked the natural endothelium. Subsequently, the specimens grown a compact cell monolayer were transferred to the new culture plates, and cultured for 8, 24, and 36 h, respectively. Finally, the absorbance of the mixture of the supernatant centrifuged by collected cell culture medium and isovolumetric Griess reagent were measured at 450 nm by a microplate reader. The detailed experimental procedure was described elsewhere.[39]

Adhesion and Proliferation of HUASMCs. Here, immunofluorescence staining of α-SMA antibodies for the HUASMCs was used to determine the cell adhesion and morphology.[39] The cell proliferation was tested by Cell Counting Kit-8 (CCK-8) method that used for the evaluation of HUVEC proliferation. The culture of HUASMCs was carried out at a density of 5×10^4 cells/cm^2, and the culture time was respectively 1, 3, and 5 days.

HUVECs and HASMCs Coculture. The coculture of HUVECs and HASMCs was performed to evaluate the cell competitive adhesion and growth behaviors. HUVECs were prelabeled with Cell Tracker Green CMFDA, while HASMCs with Orange CMTMR according to the product instructions (Molecular Probes, America). In brief, HUVECs were incubated in DMEM/F12 medium supplemented with 5 mM Cell Tracker Green CMFDA for 20 min, then washed with PBS and subsequently cultured in fresh DMEM/F12 medium free of dye for 30 min. HASMCs were labeled in the same manner except for the fluorescence dye being used, Orange CMTMR instead. Subsequently, the fluorescently labeled HUVECs and HASMCs were isolated by 0.25% trypsin-EDTA solution and centrifuged at 1200 rpm for 5 min. The cells were resuspended separately in DMEM/F12 medium with 10% fetal bovine serum to a concentration of 5×10^4 cells/mL. Finally, the HUVECs and HASMCs suspensions were mixed in a volume ratio of 1:1 and the cells were seeded at a density of 5×10^4 cells/cm^2. The competitive cell adhesion was examined after 2 and 24 h incubation in a humidified incubator at 37 °C with 5% CO_2. The cells were observed by a Leica DMRX fluorescence microscope (DMRX, Leica, Germany). The amounts of the adherent cells were calculated from at least 12 images.

Statistical Analysis. All cell experiments were performed in duplicate at least, and quantified with at least 4 replicates. XPS characterizations and QCM-D tests were performed with 3 independent repeats, and Zeta potential was carried out with 10 independent repeats. The data were presented as mean ± standard error (SD) and statistically analyzed by a one−way ANOVA using the IBM SPSS Statistics 19 software. The value of p less than 0.05 represents statistically significant difference.

3. RESULTS AND DISCUSSION

Here, XPS and IR were used to analyze the chemical composition and structure of the PPAam before and after GA conjugation. The analysis of XPS was performed to understand the changes of surface chemical compositions of the PPAam coating before and after GA immobilization. The results of XPS strongly confirmed the successful conjugation of GA, as evidenced by the visible variation in chemical compositions (see Table S1 and Figure S1 in the Supporting Information).

GA conjugation on the PPAam whether using WSC or Tris led to a substantial reduction in the peaks corresponding to nitrogen (399.5 eV) and oxygen (531.5 eV) and increase in the carbon peak (284.8 eV) (see Figure S1 in the Supporting Information). To illustrate the reaction mechanisms of GA conjugation, we further carried out C1s (Figure 1H), N1s (Figure 1I), and O1s (Figure 1J) peak fittings. Comparing the high-resolution C1s spectra of PPAam and of GA(EDC)-PPAam, a new peak at 288.4 eV occurred (Figure 1H), which was consistent with the formation of C═O/−N−C═O groups. Moreover, the conjugation of GA produced a shift of the peak at 400.6 eV in N1s spectrum (Figure 1I) toward high binding energy, which is ascribed to the presence of aromatic −N−C═O. These observations were the strong evidence of condensation reaction (active ester bonding). In the case of GA conjugation to PPAam in Tris buffer, the new peaks of terminal aromatic −COOH at 288.5 (Figure 1H) and 534 eV (Figure 1J) were detected in C1s and O1s high-resolution spectra of GA(Tris)-PPAam, respectively, and a peak at 399.5 eV was reinforced (because of the formation of aromatic C═N). This suggested the Schiff base reaction of quinone groups of GA with amine groups (in the surface of the PPAam coating). Additionally, the detection of the characteristic $-NH_3^+$ peak at 401.7 eV[40] (Figure 1I) demonstrated the existence of the salt forming reaction between −COOH of GA and $-NH_2$ of PPAam. The GATR-FTIR was performed to analyze the surface chemical structure of the substrates. As shown in Figure 2, the GA conjugation whether using Tris or WSC procedure

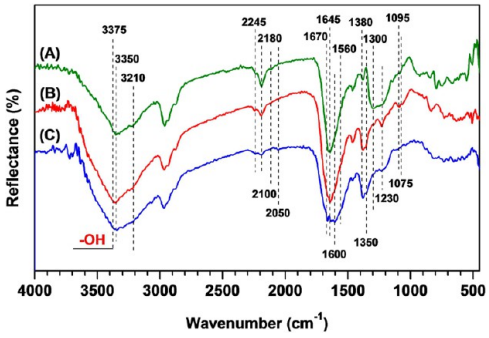

Figure 2. GATR-FTIR spectra of (A) PPAam, (B) GA(Tris)-PPAam, and (C) GA(EDC)-PPAam surfaces (see Table S2 in the Supporting Information for complete peak assignments).

produced a remarkable change in the chemical structure of PPAam. Clearly, in both GA(Tris)-PPAam and GA(EDC)-PPAam spectra, the specific peak of GA did not present in PPAam such as aromatic C═H deformation vibration (at 1095 cm^{-2}), aromatic C−O stretching and aromatic O−H deformation vibrations (at 1350 and 1260−1180 cm^{-2}), aromatic C═C stretching vibration (at 1600 cm^{-2}) and aromatic C═O stretching vibration in carboxylic acids (at 1690 cm^{-2}) were detected. In addition to this, the absorption band around 3600−3100 cm^{-2} reinforced, which was attributed to the presence of the −CO<u>OH</u> and −OH derived from GA. Note that the remarkable reinforced peak of −<u>CO</u>NH at 1670 cm^{-1} in GA(EDC)-PPAam spectrum revealed the condensation reaction between the −COOH and $-NH_2$. These observations demonstrated the immobilization of GA on substrate. The amount of GA immobilized on PPAam was tested by QCM-D. The results of QCM-D shows that after 12 h reaction and sufficient washing by PBS, the amounts of GA bound to the GA(Tris)-PPAam and GA(EDC)-PPAam were ∼395 ± 23 and ∼350 ± 29 ng/cm^2, respectively (see Figure S2 in the Supporting Information).

A regenerated healthy EC layer on vascular stent is critical to its success. The enhanced migration, adhesion, spreading, coverage, survival and proliferation, behaviors and function of ECs play crucial roles in arterial treatment and endothelium regeneration. Thus, it is very important to understand the interactions between ECs and surface. Generally, a cell adhesion process of substrate involved the attachment, spreading, cytoskeleton development, and then proliferation.[41] Hereon, the systemic evaluations for EC growth behavior were performed.

Figure 3A shows the typical fluorescence microscopic images of HUVECs. Here, cell attachment and morphology were statistically analyzed to understand the interactions of the cells with the substrate. The comparison of the numbers of cells (after 2 h culture) grown on different surface was first carried out (Figure 3B). Compared with 316L SS, the conjugation of GA leads to an increase of ∼60% in cell attachment. The remarkably enhanced cell attachment on both GA(Tris)-PPAam and GA(EDC)-PPAam surfaces revealed the strong affinity of the cells. The results of fluorescence microscopic images indicate that both GA(Tris)-PPAam and GA(EDC)-PPAam surfaces offered favorable conditions to form EC monolayer. Despite the EC spread and proliferate over time, after culture for 1 day, only ∼36% area of the 316L SS and ∼45% area of the PPAam were grown by HUVECs, while ∼73% cell area coverage was achieved on both GA functionalized surfaces (Figure 3C). After 3 days' culture, a compact monolayer of HUVECs was formed on both GA functionalized surfaces. Moreover, an insight in cellular growth behavior was gained by analysis of the projected area per cell and minor/major axis ratio (Figure 3D,E). The total projected areas of cells cultured on the GA(Tris)-PPAam and GA(EDC)-PPAam for 1 day was significant higher than those on the 316L SS and PPAam, in addition to the higher cell number. The cells grown on the GA(Tris)-PPAam and GA(EDC)-PPAam had lower minor/major ratios than those on the 316L SS and PPAam. This indicates that the GA(Tris)-PPAam and GA(EDC)-PPAam promoted cell spreading and cytoskeleton development, resulted in the more elongated cells. The elongated cells has been found to have enhanced proliferation, extracellular matrix production, and higher migrations speeds as compared to their spread out counterparts.[42,43] It is noteworthy that the projected area per cell cultured on the 316L SS and PPAam increased with the increase in cell culture time from 1 to 3 days, whereas the GA(Tris)-PPAam and GA(EDC)-PPAam presented a remarkable reduction in the projected area per cell from 2500−3000 to 2000−2400 μm^2. The too high cell density on the GA(Tris)-PPAam and GA(EDC)-PPAam after 3 day culture may be responsible for the decrease of projected area per cell, just as that reported by Puliafito et al. on the growth of epithelial cells.[44]

The evaluation of HUVEC viability, migration and function were further performed on the behalf of deduction upon the cell morphology analysis. Cell viability is a decisive factor for the subsequent cell proliferation. Here the test of apoptosis was applied to the evaluation of cell viability. As shown in Figure 4, the deposition of PPAam and further conjugation of GA to PPAam significantly enhanced the cell viability. The statistical analysis of cell viability exhibits that after culture of 1 day, only 61.4 and 76.2% of the cells survived on the control 316L SS as

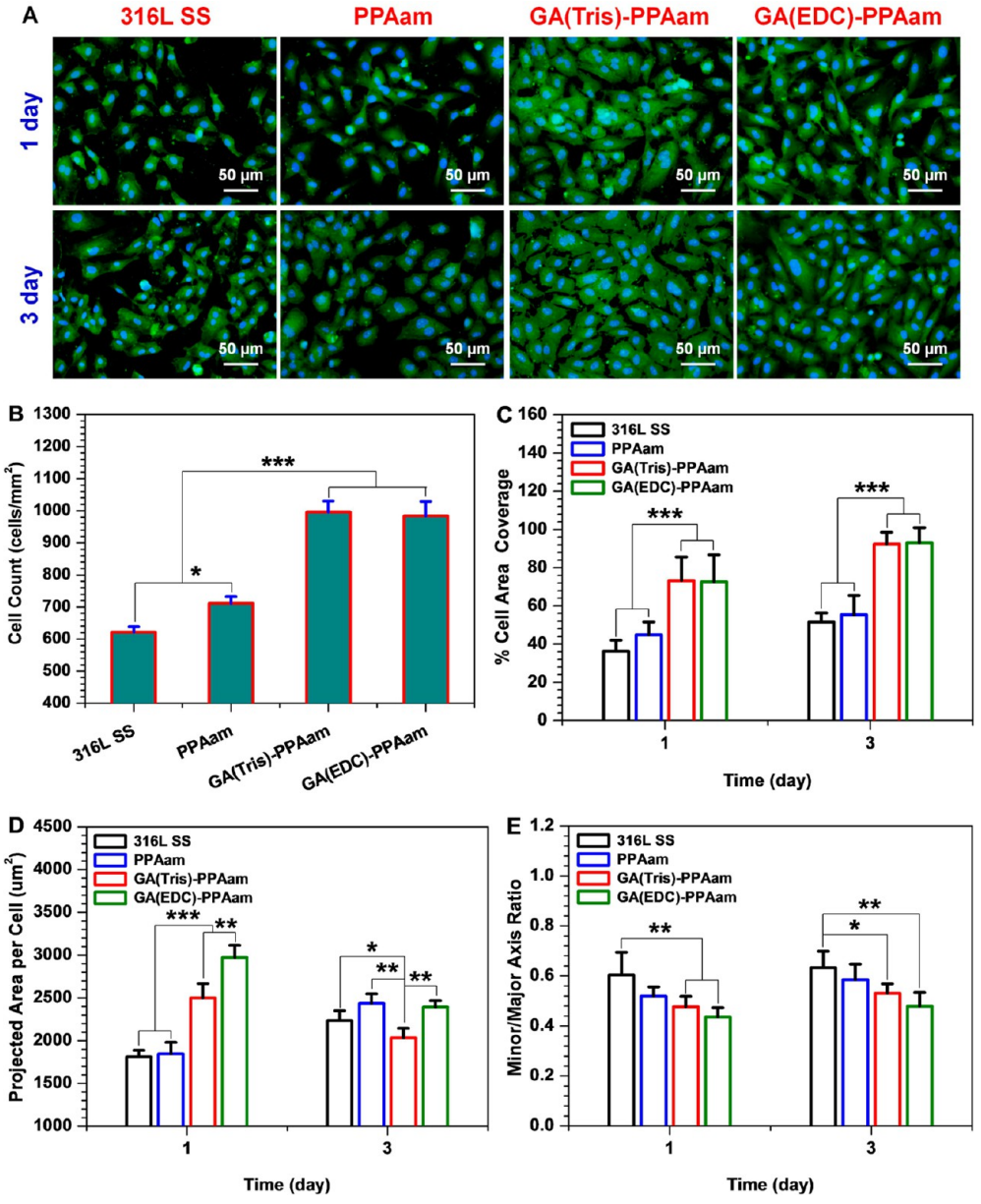

Figure 3. (A) Cytoskeletal actin (green) and nucleus (blue) stains of HUVECs on the 316L SS, PPAam, GA(Tris)-PPAam and GA(EDC)-PPAam surfaces after 1 and 3 days of culture. (B) Amounts of HUVECs attached onto different samples after cultures of 2 h are calculated from at least 12 images. (C) Surface coverage rates of the cells, (D) Projected area per cell and (E) minor/major axis ratio are calculated from at least 100 cells from six different fields based on the freehand selection of the outline of the cell using the Image J 1.43u software. Data presented as mean ± SD and analyzed using a one−way ANOVA, $*p < 0.05$, $**p < 0.01$, $***p < 0.001$.

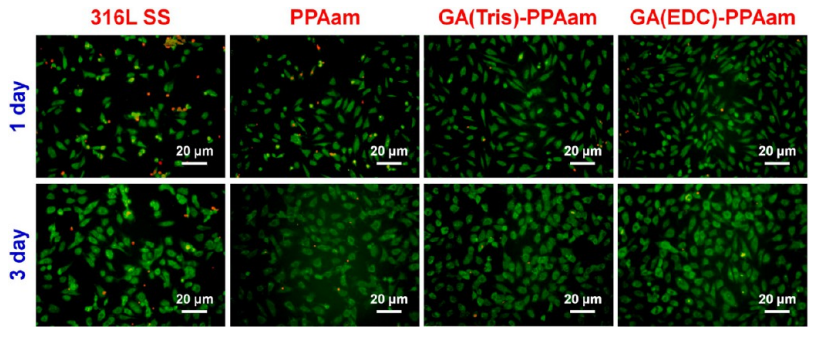

Figure 4. HUVEC adhesion and viability on 316L SS, PPAam, GA(Tris)-PPAam, and GA(EDC)-PPAam surfaces. Green, vital cells; red, dead cells.

dx.doi.org/10.1021/am405124z | ACS Appl. Mater. Interfaces 2014, 6, 2647−2656

well as PPAam substrates, while 91.2 and 92.3% of the cells were vital on the GA(Tris)-PPAam and GA(EDC)-PPAam surfaces respectively (see Figure S3 in the Supporting Information). Although the rate of vital cells increased over time on all substrates, the ratios of vital cells on both GA-PPAam surfaces was much higher than that on the 316L SS and the PPAam. As a result, both GA-PPAam surfaces showed significant promotion in the proliferation of HUVECs (Figure 5).

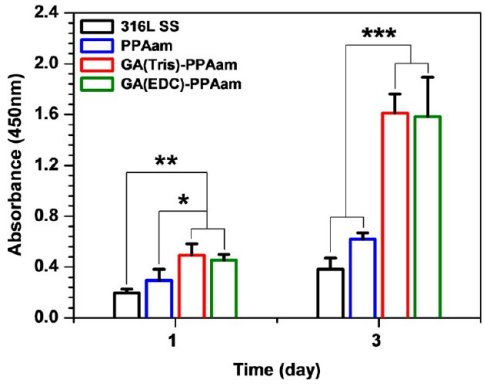

Figure 5. HUVEC proliferation cultured on 316L SS, PPAam, GA(Tris)-PPAam, and GA(EDC)-PPAam surfaces after cultures of 1 and 3 days determined by Cell Counting Kit-8. Data presented as mean ± SD and analyzed using a one−way ANOVA, $*p < 0.05$, $**p < 0.01$, $***p < 0.001$.

EC recruitment is the precondition for regeneration of endothelium. Although capturing circulating endothelial progenitor cells (EPCs) from blood played a crucial role in in situ endothelialization strategies,[45] motility of mature ECs into a lesion of the vessel wall has also attracted great interest in developing endothelium regeneration. Promoted EC migration may induce enhanced wound healing after injury or vascular stent implantation. As shown in Figure 6, the PPAam coating

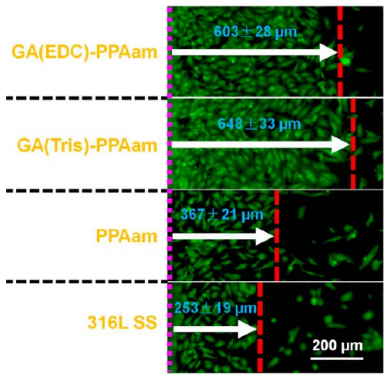

Figure 6. Migration of HUVECs on the 316L SS, PPAam, GA(Tris)-PPAam, and GA(EDC)-PPAam surfaces after 1 day culture. The migration distance was calculated from at least 12 images.

enhanced EC migration compared with the 316L SS because of the introduction of positively charged amine groups on the PPAam surface.[46] It is noteworthy that the ability of the cells to migrate on the GA(Tris)-PPAam and GA(EDC)-PPAam surfaces was significantly enhanced. The migration distance of the GA functionalized surfaces were 2.4−2.6 times the distance of the 316L SS and 1.6−1.8 times that of the PPAam. Moreover, the monolayer consisted of these migration cells was much more compact on the GA-PPAam surfaces, indicating an important effect of GA on regulating cell migration.

Healthy ECs are essential factors in maintaining vascular homeostasis. NO continuously produced by native blood vessel endothelium plays a very important role in preventing platelet activation and SMC proliferation.[47,48] Normal function of ECs grown on a stent surface is thereby crucial to its success. Hereon, the EC function was evaluated by testing the NO release per cell. As shown in Figure 7, both GA-PPAam surfaces

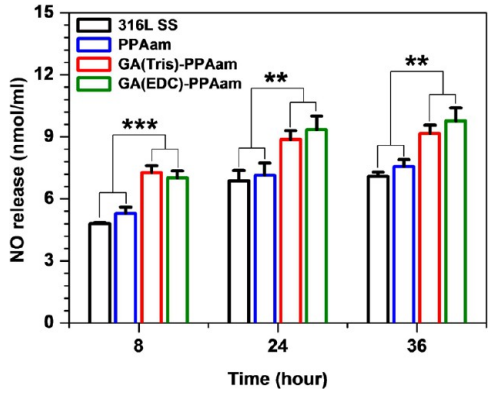

Figure 7. NO levels, measured as nitrite, released in the culture media for the 316L SS, PPAam, GA(Tris)-PPAam, and GA(EDC)-PPAam (the size of sample: Φ18 mm, $n = 4$). Data presented as mean ± SD and analyzed using a one-way ANOVA, $*p < 0.05$, $**p < 0.01$.

remarkably promoted the release of NO. The enhancement of NO production fits the demands of ideal stent. The above data indicate that GA-PPAam surfaces provided a favorable microenvironment for HUVEC growth.

The implantation of a stent may provoke a cascade of cellular and biochemical responses that induce pathological processes, such as thrombosis and cytokine release. These pathological complications subsequently trigger VSMC proliferation, hence result in in-stent restenosis (ISR).[49−51] Therefore, the inhibition of proliferation VSMCs can effectively reduce ISR rate. In this work, VSMC growth responses to GA-PPAam coatings were studied through immunostaining and testing of HUASMC proliferation. Viability (see Figure S4 in the Supporting Information), morphology (Figure 8), and proliferation (Figure 9) show that the GA-PPAam coatings significantly inhibited adhesion, viability, and proliferation of HUASMCs with serum stimulation. It is noteworthy that the GA(Tris)-PPAam presented stronger inhibitory effects in HUASMC proliferation (Figure 9) and greater ability to induce apoptosis of HUASMCs (see Figure S4 in the Supporting Information) than the GA(EDC)-PPAam.

The mechanism by which GA interacts with human endothelial cells has been reported to mainly involve in the effect on NO production of ECs. Some researchers have reported that polyphenols might promote attachment of ECs and endothelial NO production. Cocks and Kubota et al.[30,31] have found that the enhanced endothelial NO production by polyphenols was based on indirect increase of intracellular Ca^{2+} levels. However, others reported effects of GA on NO release showed conflicting results.[52−55] For instance, Huisman et al.[52] have found that wine polyphenols including GA exhibited indistinctive effects on endothelial nitric oxide production. These reported contradictive results may be ascribed to the use

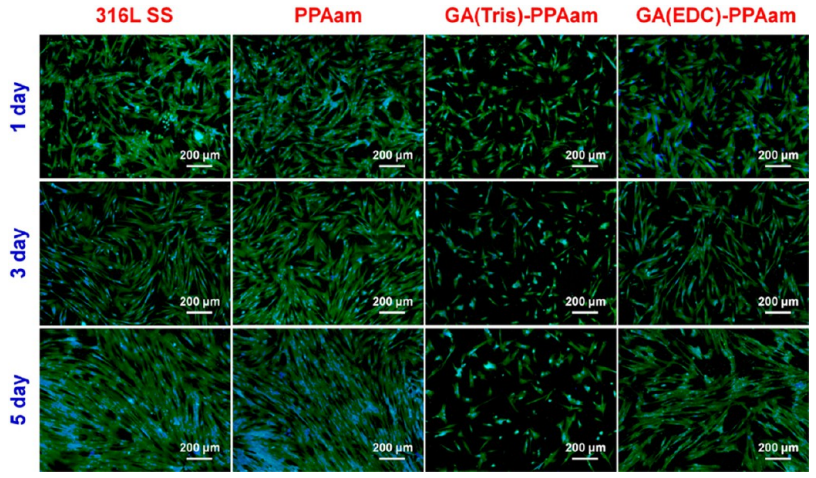

Figure 8. Immunofluorescence staining of HUASMCs grown onto the 316L SS, PPAam, GA(Tris)-PPAam, and GA(EDC)-PPAam surfaces.

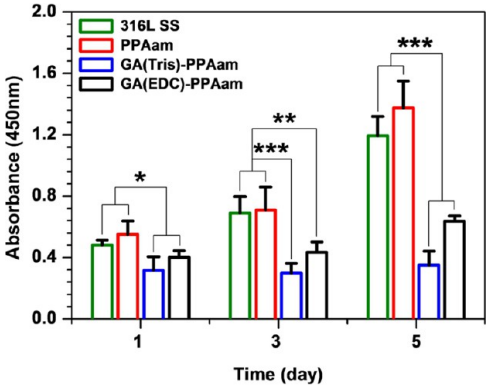

Figure 9. HUASMC proliferation on 316L SS, PPAam, GA(Tris)-PPAam, and GA(EDC)-PPAam surfaces after 1, 3, and 5 days' culture. Data presented as mean ± SD and analyzed using a one−way ANOVA, $^{**}p < 0.01$ and $^{***}p < 0.001$.

of different concentration of GA in cell culture medium. GA is a negatively charged molecule (see Table S2 in the Supporting Information), it is thereby unlikely to permeate cell. It is conceivable that the effects of GA on cells should base on the reaction of GA with cell membrane.[28] Yang et al.[56] have reported that the effects of GA on ECs was strongly relied on the GA concentration in cell culture medium. In this work, the amount of GA conjugated to PPAam coating was about 400 ng/cm^2. The significant enhancement in HUVEC attachment, proliferation, viability, migration and NO release observed in this work may confirm this as a suitable concentration of GA bound to the PPAam. In addition to the effect of GA on NO release, Ku et al.[57] reported that the phenolic hydroxyl group could facilitate the adsorption of serum proteins, which serve as adhesion sites for ECs. Our results show that GA-PPAam could bind more fetal bovine serum (FBS) than 316L SS and control PPAam coating (see Figure S5 in the Supporting Information), which may significantly contribute to the enhanced EC attachment.

Suppression of VSMC proliferation is a very important aspect for improving the performance of a stent. In this work, GA-PPAam coatings showed substantial inhibition in adhesion, viability, and proliferation of HUASMCs. Till now, very few studies focused on the growth behavior of GA on VSMC. Oxidative stress by reactive oxygen species of ·OH produced by GA has been recognized to be one of the most important mechanism of GA-induced death of VSMCs.[28] In this work, although the coupling procedure and amount of GA conjugated to PPAam coating were different, there was no significant difference in the effects on HUVEC growth, whereas there was remarkable difference in morphology, viability and proliferation of HUASMCs. The GA(Tris)-PPAam coating presented a stronger inhibitory effect on HUASMC proliferation than the GA(EDC)-PPAam. Epigallocatechin-3-*O*-gallate (EGCG) is a derivative of GA and shows the very similar functional groups as GA) (see Figure S6 in the Supporting Information). Many reports on the study of EGCG on VSMCs revealed that EGCG exhibited substantial inhibitory effects, which are ascribed to existence of the galloyl group and phenolic hydroxyl groups.[32−34] Moreover, some investigations of catechins on VSMCs found that the galloyl group of the catechin is essential to full inhibitory activity for SMCs.[35−37] Note that both galloyl group in the 3-position and phenolic hydroxyl groups are presented on the GA(Tris)-PPAam coating, whereas only phenolic hydroxyl groups and no galloyl group is retained on the GA(EDC)-PPAam coating. Our observations of the inhibitory effects of GA on VSMCs strongly confirm the reported results. The mechanism by which catechins with galloyl and phenolic hydroxyl groups inhibits VSMC migration and proliferation has been widely reported. Stangl and Rodriguez et al.[19,58] suggested that the binding of EGCG at specific sites on the cellular membrane affect the DNA replication and cell proliferation might cause the inhibitory effects. Han et al.[59] showed that EGCG inhibits serum-stimulated rat aortic smooth muscle cells by down-regulating nuclear factor-κB. Kim et al.[60] found that the EGCG-induced vascular SMC arrest is ascribed to suppress cyclin D1/CDK4 and cyclin E/CDK2 complexes that regulate G1 to S cell cycle progression. The finding of EGCG on SMC growth behavior indirectly serve as some explanation on the different degree of the effects on HUASMCs produced by GA(Tris)-PPAam and GA(EDC)-PPAam. Although a low density of 400 ng/cm^2 of GA (relative to reported several ug/mL) was immobilized on the PPAam, it showed significant inhibitory effect on SMCs. This may be the evidence for supporting the above deduction that is the effects of GA on cell take place at or near the cell membrane.

The inhibitory effects of DES on the proliferation of ECs have drawn the focus of research on enhancing rapid re-

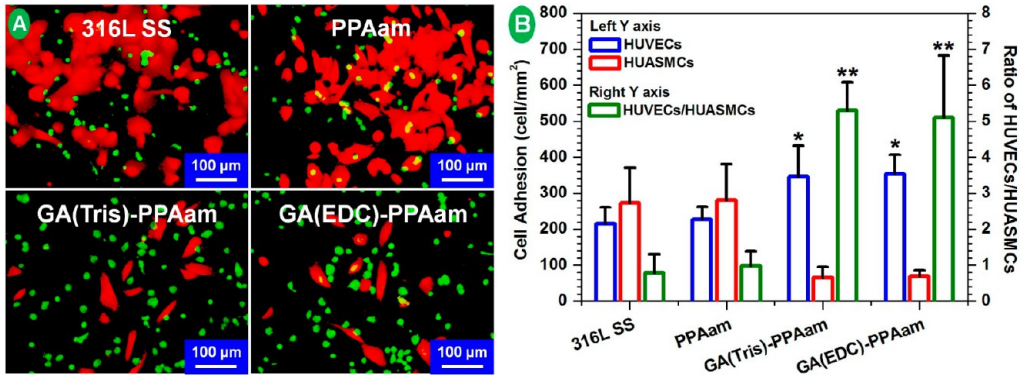

Figure 10. (A) Immunofluorescence staining of HUVECs (green) and HUASMCs (red) grown onto the 316L SS, PPAam, GA(Tris)-PPAam, and GA(EDC)-PPAam surfaces after coculture for 2 h. (B) Number of cells grown onto the surfaces is calculated by at least six images. Data presented as mean ± SD and analyzed using a one-way ANOVA, $*p < 0.05$ (HUVEC vs HUASMCs) and $**p < 0.01$ (vs 316L SS and PPAam). The right *Y* axis with bias columns shows the ratio of the number of HUVECs to the number HUASMCs.

endothelialization by immobilized biomolecules. Unfortunately, unsatisfactory clinical results have been reported.[61,62] This may be attributed to the ignorance of the competitive growth of ECs and SMCs in vivo. Some recent studies demonstrated that the competitive ability of ECs over SMCs played the more important role than the amount of the adherent ECs in the formation of a new pure endothelial layer in vivo and prevention of restenosis.[63,64] Herein, the competitive adhesion of vascular cells was further evaluated. As shown in Figure 10A and Figure S7 in the Supporting Information, clearly, both GA(Tris)-PPAam and GA(EDC)-PPAam showed the unique character of selectively promoting EC growth while inhibiting SMC adhesion and proliferation. The number of cells grown on each specimen was further calculated from fluorescence micrographs for the statistical analysis. After 2 h showed the number of HUVECs adherent on GA(Tris)-PPAam or GA(EDC)-PPAam was about 1.5-times higher than on 316L SS or PPAam, but the number of HUASMCs on GA(Tris)-PPAam or GA(EDC)-PPAam was only about 25% of that on 316L SS or PPAam (Figure 10B). The ratio of HUVECs to HUASMCs of the GA(Tris)-PPAam and GA(EDC)-PPAam were 5.3 and 5.1 respectively, which were greatly higher than that of the 316L SS (0.79) and of the PPAam (0.97). The excellent competitive ability of HUVECs over HUASMCs on GA-PPAam surfaces suggested the possibility in forming a pure endothelial layer on stent in vivo.

4. CONCLUSIONS

We have reported a simple technique of GA coating that on a PPAam surface to tailor surface functionalities. By application of this technique as vascular stent coating, the behavior of blood vessel cells, smooth muscle cells, and endothelium could be selectively directed. The GA-PPAam coating presented strongly selective effects on vascular cells, as evidenced by the substantial enhancement in attachment, proliferation, viability, migration, and function of HUVECs, and significant inhibition in HUASMC adhesion and proliferation. These unique functionalities of the GA-PPAam coating suggest the potential application in the construction of an ideal stent platform for addressing the issues of restenosis.

■ ASSOCIATED CONTENT

Supporting Information

Scheme S1 for the schematic illustration of HUVEC migration assay; Table S1 and Figure S1 for the chemical compositions of the PPAam, GA(Tris)-PPAam, and GA(EDC)-PPAam coatings; Figure S2 for the amount of GA conjugated on the PPAam real time monitored by QCM-D; Figure S3 for the ratios of vital HUVECs grown on the 316L SS, PPAam, GA(Tris)-PPAam, and GA(EDC)-PPAam coatings; Figure S4 for the HUASMC viability onto the 316L SS, PPAam, GA(Tris)-PPAam, and GA(EDC)-PPAam surfaces; Figure S5 for the amounts of FBS bound to the different surfaces real time monitored by QCM-D; Figure S7 for the immunofluorescence staining of HUVECs (green) and HUASMCs (red) grown onto the 316L SS, PPAam, GA(Tris)-PPAam, and GA(EDC)-PPAam surfaces after coculture for 1 day; Table S2 for the zeta potential of the 316L SS, PPAam, and GA-PPAam coatings. This material is available free of charge via the Internet at http://pubs.acs.org.

■ AUTHOR INFORMATION

Corresponding Authors

*E-mail: zhiluyang1029@126.com. Tel: +86 28 87600625. Fax: +86 28 87600625.
*E-mail: jinxxwang@263.net.
*E-mail: nhuang@263.net

Notes

The authors declare no competing financial interest.

■ ACKNOWLEDGMENTS

This work was supported by the NSFC (Project 81271701 and 51173149), the Ministry of Science and Technology of China (Key Basic Research Project 2011CB606204), and NSFC Key Program 81330031. We thank Miss Xue Lin for providing the photos of Figure 1 A, B, and thank Manfred F. Maitz for revising the manuscript.

■ REFERENCES

(1) Shuchman, M. N. Trading Restenosis for Thrombosis? New Questions about Drug-Eluting Stents. *New Engl. J. Med.* **2006**, *355*, 1949−1955.
(2) Tsimikas, S. Drug-Eluting Stents and Late Adverse Clinical Outcomes Lessons Learned, Lessons Awaited. *J. Am. Coll. Cardiol.* **2006**, *47*, 2112−2115.

(3) Zilberman, M.; Eberhart, R. C. Drug-Eluting Bioresorbable Stents for Various Applications. *Annu. Rev. Biomed. Eng.* **2006**, *8*, 153−180.
(4) Eisenberg, M. J.; Konnyu, K. J. Review of Randomized Clinical Trials of Drug-Eluting Stents for the Prevention of In-Stent Restenosis. *Am. J. Cardiol.* **2006**, *98*, 375−382.
(5) Tsuchida, K.; Serruys, P. W.; Bruining, N.; Dudek, D.; Drzewiecki, J.; Banning, A. P. Two-Year Serial Coronary Angiographic and Intravascular Ultrasound Analysis of In-Stent Angiographic Late Lumen Loss and Ultrasonic Neointimal Volume from the TAXUS II Trial. *Am. J. Cardiol.* **2007**, *99*, 607−615.
(6) Cutlip, D. E.; Baim, D. S.; Ho, K. K. L.; Popma, J. J.; Lansky, A. J.; Cohen, D. J. Stent Thrombosis in the Modern Era: A Pooled Analysis of Multicenter Coronary Stent Clinical Trials. *Circulation* **2001**, *103*, 1967−1971.
(7) Finn, A. V.; Joner, M.; Nakazawa, G.; Kolodgie, F.; Newell, J.; John, M. C. Pathological Correlates of Late Drug-Eluting Stent Thrombosis: Strut Coverage As a Marker of Endothelialization. *Circulation* **2007**, *115*, 2435−2441.
(8) Kerdjoudj, H.; Boura, C.; Moby, V.; Montagne, K.; Schaaf, P.; Voegel, J. C. Re-endothelialization of Human Umbilical Arteries Treated with Polyelectrolyte Multilayers: A Tool for Damaged Vessel Replacement. *Adv. Funct. Mater.* **2007**, *17*, 2667−2673.
(9) Pernagallo, S.; Tura, O.; Wu, M.; Samuel, K.; Diaz-Mochon, J. J.; Hansen, A. Novel Biopolymers to Enhance Endothelialisation of Intra-Vascular Devices. *Adv. Healthcare Mater.* **2012**, *1*, 646−656.
(10) Yang, Z. L.; Tu, Q. F.; Zhu, Y.; Luo, R. F.; Li, X.; Xie, Y. C. Mussel-Inspired Coating of Polydopamine Directs Endothelial and Smooth Muscle Cell Fate for Re-endothelialization of Vascular Devices. *Adv. Healthcare Mater.* **2012**, *1*, 548−559.
(11) Müller, S.; Koenig, G.; Charpiot, A.; Debry, C.; Voegel, J. C.; Lavalle, P. VEGF-Functionalized Polyelectrolyte Multilayers as Proangiogenic Prosthetic Coatings. *Adv. Funct. Mater* **2008**, *18*, 1767−1775.
(12) Yin, Y.; Wise, S. G.; Nosworthy, N. J.; Waterhouse, A.; Bax, D. V.; Youssef, H. Covalent Immobilisation of Tropoelastin on a Plasma Deposited Interface for Enhancement of Endothelialisation on Metal Surfaces. *Biomaterials* **2009**, *30*, 1675−1781.
(13) Yin, M.; Yuan, Y.; Liu, C.; Wang, J. Development of Mussel Adhesive Polypeptide Mimics Coating for In-Situ Inducing Re-endothelialization of Intravascular Stent Devices. *Biomaterials* **2009**, *30*, 2764−2773.
(14) Peng, L. L.; Eltgroth, M. L.; LaTempa, T. J.; Grimes, C. A.; Desai, T. A. The Effect of TiO_2 Nanotubes on Endothelial Function and Smooth Muscle Proliferation. *Biomaterials* **2009**, *30*, 1268−1272.
(15) Smith, B. S.; Yoriya, S.; Grissom, L.; Grimes, C. A.; Popat, K. C. Hemocompatibility of Titania Nanotube Arrays. *J. Biomed. Mater. Res.* **2010**, *95A*, 350−360.
(16) Waterhouse, A.; Yin, Y. B.; Wise, S. G.; Bax, D. V.; McKenzie, D. R.; Bilek, M. M. M. The Immobilization of Recombinant Human Tropoelastin on Metals using a Plasma-Activated Coating to Improve the Biocompatibility of Coronary Stents. *Biomaterials* **2010**, *31*, 8332−8340.
(17) Yang, Z. L.; Wang, J.; Luo, R. F.; Maitz, M. F.; Jing, F. J.; Sun, H.; Huang, N. The Covalent Immobilization of Heparin to Pulsed-Plasma Polymeric Allylamine Films on 316L Stainless Steel and the Resulting Effects on Hemocompatibility. *Biomaterials* **2010**, *31*, 2072−83.
(18) Waterhouse, A.; Wise, S. G.; Yin, Y. B.; Wu, B. C.; James, B.; Zreiqat, H. In Vivo Biocompatibility of a Plasma-Activated, Coronary Stent Coating. *Biomaterials* **2012**, *33*, 7984−7992.
(19) Stangl, V.; Dreger, H.; Stangl, K.; Lorenz, M. Molecular Targets of Tea Polyphenols in the Cardiovascular System. *Cardiovasc. Res.* **2007**, *73*, 348−358.
(20) Ho, C. T.; Chen, Q.; Shi, H.; Zhang, K. Q.; Rosen, R. T. Antioxidative Effect of Polyphenol Extract Prepared from Various Chinese Teas. *Prev. Med.* **1992**, *21*, 520−525.
(21) Caccetta, R. A. A.; Burke, V.; Mori, T. A.; Beilin, L. J.; Puddey, I. B.; Croft, K. D. Red Wine Polyphenols, in the Absence of Alcohol, Reduce Lipid Peroxidative Stress in Smoking Subjects. *Free Radical Biol. Med.* **2001**, *30*, 636−642.
(22) Kang, M. S.; Oh, J. S.; Kang, I. C.; Hong, S. J.; Choi, C. H. Inhibitory Effect of Methyl Gallate and Gallic Acid on Oral Bacteria. *J. Microbiol.* **2008**, *46*, 744−50.
(23) Kratz, J. M.; Andrighetti-Frohner, C. R.; Leal, P. C.; Nunes, R. J.; Yunes, R. A.; Trybala, E. Evaluation of Anti-HSV-2 Activity of Gallic Acid and Pentyl Gallate. *Biol. Pharm. Bull.* **2008**, *31*, 903−907.
(24) Kim, S. H.; Jun, C. D.; Suk, K.; Choi, B. J.; Lim, H.; Park, S. Gallic Acid Inhibits Histamine Release and Pro-Inflammatory Cytokine Production in Mast Cells. *Toxicol. Sci.* **2006**, *91*, 123−131.
(25) Urizzi, P.; Monje, M. C.; Souchard, J. P.; Abella, A.; Chalas, J.; Lindenbaum, A. Antioxidant Activity of Phenolic Acids and Esters Present in Red Wine on Human Low-Density Lipoproteins. *J. Chim. Phys.* **1999**, *96*, 110−115.
(26) Chen, H. M.; Wu, Y. C.; Chia, Y. C.; Chang, F. R.; Hsu, H. K.; Hsieh, Y. C. Gallic Acid, a Major Component of Toona Sinensis Leaf Extracts, Contains a ROS-Mediated Anti-Cancer Activity in Human Prostate Cancer Cells. *Cancer Lett.* **2009**, *286*, 161−171.
(27) Inoue, M.; Sakaguchi, N.; Isuzugawa, K.; Tani, H.; Ogihara, Y. Role of Reactive Oxygen Species in Gallic Acid-Induced Apoptosis. *Biol. Pharm. Bull.* **2000**, *23*, 1153−1157.
(28) Qiu, X. B.; Takemura, G.; Koshiji, M.; Hayakawa, Y.; Kanoh, M.; Maruyama, R. Gallic Acid Induces Vascular Smooth Muscle Cell Death via Hydroxyl Radical Production. *Heart Vessels* **2000**, *15*, 90−99.
(29) Inoue, M.; Suzuki, R.; Sakaguchi, N.; Li, Z.; Takeda, T.; Ogihara, Y. Selective Induction of Cell Death in Cancer Cells by Gallic Acid. *Biol. Pharm. Bull.* **1995**, *18*, 1526−30.
(30) Cocks, T. M.; Angus, J. A.; Campbell, J. H.; Campbell, G. R. Release and Properties of Endothelium-Derived Relaxing Factor (EDRF) from Endothelial Cells in Culture. *J. Cell. Physiol.* **1985**, *123*, 310−320.
(31) Kubota, Y.; Tanaka, N.; Umegaki, K.; Takenaka, H.; Mizuno, H.; Nakamura, K. Ginkgo Biloba Extract-Induced Relaxation of Rat Aorta is Associated with Increase in Endothelial Intracellular Calcium Level. *Life Sci.* **2001**, *69*, 2327−2236.
(32) Cheng, X. W.; Kuzuya, M.; Nakamura, K.; Liu, Z.; Di, Q.; Hasegawa, J. Mechanisms of the Inhibitory Effect of Epigallocatechin-3-Gallate on Cultured Human Vascular Smooth Muscle Cell Invasion. *Arterioscler. Thromb. Vasc. Biol.* **2005**, *25*, 1864−1870.
(33) Isemura, M.; Saeki, K.; Kimura, T.; Hayakawa, S.; Minami, T.; Sazuka, M. Tea Catechins and Related Polyphenols as Anti-Cancer Agents. *Biofactors* **2000**, *13*, 81−85.
(34) Sachinidis, A.; Skach, R. A.; Seul, C.; Ko, Y.; Hescheler, J.; Ahn, H.-Y. Inhibition of the PDGF B-Receptor Tyrosine Phosphorylation and its Downstream Intracellular Signal Transduction Pathway in Rat and Human Vascular Smooth Muscle Cells by Different Catechins. *FASEB J.* **2002**, *16*, 893−895.
(35) Kim, D. W.; Park, Y. S.; Kim, Y. G.; Piao, H.; Kwon, J. S.; Hwang, K. K. Local Delivery of Green Tea Catechins Inhibits Neointimal Formation in the Rat Carotid Artery Injury Model. *Heart Vessels* **2004**, *19*, 242−247.
(36) Lu, L. H.; Lee, S. S.; Huang, H. C. Epigallocatechin Suppression of Proliferation of Vascular Smooth Muscle Cells: Correlation with C-Jun and JNK. *Br. J. Pharmacol.* **1998**, *24*, 1227−1237.
(37) Chyu, K. Y.; Babbidge, S. M.; Zhao, X.; Dandillaya, R.; Rietveld, A. G.; Yano, J. Differential Effects of Green Tea-Derived Catechin on Developing Versus Established Atherosclerosis in Apolipoprotein E-Null Mice. *Circulation* **2004**, *109*, 2448−2453.
(38) Yang, Z. L.; Wang, X. N.; Wang, J.; Yao, Y.; Sun, H.; Huang, N. Pulsed-Plasma Polymeric Allylamine Thin Films. *Plasma Process Polym.* **2009**, *6*, 498−505.
(39) Yang, Z. L.; Tu, Q. F.; Wang, J.; Huang, N. The Role of Heparin Binding Surfaces in the Direction of Endothelial and Smooth Muscle Cell Fate and Re-endothelialization. *Biomaterials* **2012**, *33*, 6615−6625.
(40) Yang, Z. L.; Lei, X. J.; Wang, J.; Luo, R. F.; He, T. T.; Sun, H.; Huang, N. A Novel Technique toward Bipolar Films Containing Alternating Nanolayers of Allylamine and Acrylic Acid Plasma

Polymers for Biomedical Application. *Plasma Process Polym.* **2011**, *8*, 208−214.
(41) Hersel, U.; Dahmen, C.; Kessler, H. RGD Modified Polymers: Biomaterials for Stimulated Cell Adhesion and Beyond. *Biomaterials* **2003**, *24*, 4382−415.
(42) Tanaka, M.; Takayama, A.; Ito, E.; Sunami, H.; Yamamoto, S.; Shimomura, M. Effect of Pore Size of Self-Organized Honeycomb-Patterned Polymer Films on Spreading, Focal Adhesion, Proliferation, and Function of Endothelial Cells. *J. Nanosci. Nanotechnol.* **2007**, *7*, 763−772.
(43) McGrath, J. L.; Osborn, E. A.; Tardy, Y. S.; Dewey, C. F., Jr.; Hartwig, J. H. Regulation of the Actin Cycle in vivo by Actin Filament Severing. *Proc. Natl. Acad. Sci. U.S.A.* **2000**, *97*, 6532−6527.
(44) Puliafitoa, A.; Hufnagel, L.; Neveu, P.; Streichan, S.; Sigal, A.; Fygenson, D. K.; Shraiman, B. I. Collective and Single Cell Behavior in Epithelial Contact Inhibition. *Proc. Natl. Acad. Sci. U.S.A.* **2012**, *17*, 739−744.
(45) Avci-Adali, M.; Ziemer, G.; Wendel, H. Induction of EPC Homing on Biofunctionalized Vascular Grafts for Rapid in vivo Self-endothelialization—A Review of Current Strategies. *Biotechnol Adv.* **2010**, *28*, 119−129.
(46) Yang, Z. L.; Tu, Q. F.; Wang, J.; Lei, X. J.; He, T. T.; Sun, H.; Huang, N. Bioactive Plasma Polymerized Bipolar Films for Enhanced Endothelial Cell Mobility. *Macromol. Biosci.* **2011**, *11*, 797−805.
(47) McCormick, C.; Wadsworth, R. M.; Jones, R. L.; Kennedy, S. Prostacyclin Analogues: The Next Drug-Eluting Stent? *Biochem. Soc. Trans.* **2007**, *35*, 910−911.
(48) Sneddon, J. M.; Vane, J. R. Endothelium-Derived Relaxing Factor Reduces Platelet Adhesion to Bovine Endothelial Cells. *Proc. Natl. Acad. Sci. U.S.A.* **1988**, *85*, 2800−2804.
(49) Garas, S. M.; Huber, P.; Scott, N. A. Overview of Therapies for Prevention of Restenosis after Coronary Interventions. *Pharmacol. Ther.* **2001**, *92*, 165−178.
(50) Rajagopal, V.; Rockson, S. G. Coronary Restenosis: A Review of Mechanisms and Management. *Am. J. Med.* **2003**, *115*, 547−553.
(51) Bennett, M. R.; O'Sullivan, M. Mechanisms of Angioplasty and Stent Restenosis: Implications for Design of Rational Therapy. *Pharmacol. Ther.* **2001**, *91*, 149−166.
(52) Huisman, A.; van de Wiel, A.; Rabelink, T. J.; van Faassen, E. E. Wine Polyphenols and Ethanol Do Not Significantly Scavenge Superoxide Nor Affect Endothelial Nitric Oxide Production. *J. Nutr. Biochem.* **2004**, *15*, 426−432.
(53) Huang, Y.; Chan, N. W. K.; Lau, C. W.; Yao, X. Q.; Chan, F. L.; Chen, Z. Y. Involvement of Endothelium/Nitric Oxide in Vaso-relaxation Induced by Purified Green Tea (—) Epicatechin. *Biochim. Biophys. Acta* **1999**, *1427*, 322−328.
(54) Benito, S.; Lopez, D.; Saiz, M. P.; Buxaderas, S.; Sanchez, J.; Puig-Parellada, P. A Flavonoid-Rich Diet Increases Nitric Oxide Production in Rat Aorta. *Br. J. Pharmacol.* **2002**, *135*, 910−916.
(55) Furchgott, R. F. Role of Endothelium in Responses of Vascular Smooth Muscle. *Circ. Res.* **1983**, *53*, 557−573.
(56) Yang, H. L.; Chen, S. C.; Lin, K. Y.; Wang, M. T.; Chen, Y. C.; Huang, H. C. Antioxidant Activities of Aqueous Leaf Extracts of Toona Sinensis on Freeradical-Induced Endothelial Cell Damage. *J. Ethnopharmacol.* **2011**, *137*, 669−680.
(57) Ku, S. H.; Ryu, J.; Hong, S. K.; Lee, H.; Park, C. B. General Functionalization Route for Cell Adhesion on Non-Wetting Surfaces. *Biomaterials* **2010**, *31*, 2535−2541.
(58) Rodriguez, S. K.; Guo, W.; Liu, L.; Band, M. A.; Paulson, E. K.; Meydani, M. Green Tea Catechin, Epigallocatechin-3-Gallate, Inhibits Vascular Endothelial Growth Factor Angiogenic Signaling by Disrupting the Formation of a Receptor Complex. *Int. J. Cancer* **2006**, *118*, 1635−1644.
(59) Han, D. W.; Lim, H. R.; Baek, H. S.; Lee, M. H.; Lee, S. J.; Hyon, S. H. Inhibitory Effects of Epigallocatechin-3-O-Gallate on Serum-Stimulated Rat Aortic Smooth Muscle Cells via Nuclear Factor-κB Down-Modulation. *Biochem. Biopharm. Res. Commun.* **2006**, *345*, 148−155.
(60) Kim, C. H.; Moon, S. K. Epigallocatechin-3-Gallate Causes the p21/WAF1-Mediated G(1)-Phase Arrest of Cell Cycle and Inhibits Matrix Metalloproteinase-9 Expression in TNF-Alpha-Induced Vascular Smooth Muscle Cells. *Arch. Biochem. Biophys.* **2005**, *435*, 264−272.
(61) Aoki, J.; Serruys, P. W.; van Beusekom, H.; Ong, A. T. L.; McFadden, E. P.; Sianos, G. Endothelial Progenitor Cell Capture by Stents Coated with Antibody Against CD34: The HEALING-FIM (Healthy Endothelial Accelerated Lining Inhibits Neointimal Growth-First In Man) Registry. *J. Am. Coll. Cardiol.* **2005**, *45*, 1574−1579.
(62) Hill, J. M.; Zalos, G.; Halcox, J. P. J.; Schenke, W. H.; Waclawiw, M. A.; Quyyumi, A. A.; Finkel, T. Circulating Endothelial Progenitor Cells, Vascular Function, and Cardiovascular Risk. *New Engl. J. Med.* **2003**, *348*, 593−600.
(63) Ceylan, H.; Tekinay, A. B.; Guler, M. O. Selective Adhesion and Growth of Vascular Endothelial Cells on Bioactive Peptide Nanofiber Functionalized Stainless Steel Surface. *Biomaterials* **2011**, *32*, 8797−8805.
(64) Wei, Y.; Ji, Y.; Xiao, L. L.; Lin, Q. K.; Xu, J. P.; Ren, K. F.; Ji, J. Surface Engineering of Cardiovascular Stent with Endothelial Cell Selectivity for in vivo Re-endothelialisation. *Biomaterials* **2013**, *34*, 2588−2599.